Structural and functional analyses of the DMC1-M200V polymorphism found in the human population

Juri Hikiba, Kouji Hirota, Waturu Kagawa, Shukuko Ikawa, Takashi Kinebuchi, Isao Sakane, Yoshimasa Takizawa, Shigeyuki Yokoyama, Béatrice Mandon-Pepin, Alain Nicolas, et al.

HAL Id: hal-02659900

https://hal.inrae.fr/hal-02659900

Submitted on 30 May 2020

Structural and functional analyses of the DMC1-M200V polymorphism found in the human population

Juri Hikiba[1], Kouji Hirota[2,3], Wataru Kagawa[4], Shukuko Ikawa[3], Takashi Kinebuchi[4], Isao Sakane[5], Yoshimasa Takizawa[1], Shigeyuki Yokoyama[4,6], Béatrice Mandon-Pépin[7], Alain Nicolas[8], Takehiko Shibata[3], Kunihiro Ohta[2,3] and Hitoshi Kurumizaka[1,4,5,*]

[1]Laboratory of Structural Biology, Graduate School of Advanced Science and Engineering, Waseda University, 2-2 Wakamatsu-cho, Shinjuku-ku, Tokyo 162-8480, [2]Department of Life Sciences, Graduate School of Arts and Sciences, The University of Tokyo, 3-8-1 Komaba, Meguro-ku, Tokyo 153-8902, [3]RIKEN Advanced Research Institute, 2-1 Hirosawa, Wako-shi, Saitama 351-0198, [4]RIKEN Systems and Structural Biology Center, 1-7-22 Suehiro-cho, Tsurumi, Yokohama-shi, Kanagawa 230-0045, [5]Institute for Biomedical Engineering, Consolidated Research Institute for Advanced Science and Medical Care, Waseda University, 513 Wasedatsurumaki-cho, Shinjuku-ku, Tokyo 162-0041, [6]Department of Biophysics and Biochemistry, Graduate School of Science, The University of Tokyo, 7-3-1 Hongo, Bunkyo-ku, Tokyo 113-0033, Japan, [7]INRA, UMR1198; ENVA; CNRS; FRE 2857, Biologie du Developpement et Reproduction, Jouy-en-Josas, F-78350 and [8]Institut Curie, Centre de Recherche, UMR7147 - Centre National de la Recherche Scientifique, Université Pierre et Marie Curie, 26 rue d'Ulm, 75248 Paris Cedex 05, France

ABSTRACT

The M200V polymorphism of the human DMC1 protein, which is an essential, meiosis-specific DNA recombinase, was found in an infertile patient, raising the question of whether this homozygous *human DMC1-M200V* polymorphism may cause infertility by affecting the function of the human DMC1 protein. In the present study, we determined the crystal structure of the human DMC1-M200V variant in the octameric-ring form. Biochemical analyses revealed that the human DMC1-M200V variant had reduced stability, and was moderately defective in catalyzing *in vitro* recombination reactions. The corresponding M194V mutation introduced in the *Schizosaccharomyces pombe dmc1* gene caused a significant decrease in the meiotic homologous recombination frequency. Together, these structural, biochemical and genetic results provide extensive evidence that the human DMC1-M200V mutation impairs its function, supporting the previous interpretation that this single-nucleotide polymorphism is a source of human infertility.

INTRODUCTION

In meiosis, a physical connection between homologous chromosomes is established by homologous recombination (meiotic recombination) to ensure proper chromosome segregation (1,2). Meiotic recombination is initiated by the formation of double-strand breaks (DSBs) by the Spo11 protein in one of the homologous chromosomes, and then the 3′ single-stranded DNA (ssDNA) tails are enzymatically generated at the DSB sites (3–5). The ssDNA tail assimilates into the double-stranded DNA (dsDNA) of the other, intact homologous chromosome, to form a short stretch of new Watson–Crick base pairs between the invading strand and its complementary strand of parental dsDNA (homologous pairing) (6,7). After this homologous-pairing reaction, the heteroduplex formed between homologous chromosomes is expanded by the subsequent strand-exchange reaction (6,7). The *Escherichia coli* RecA protein catalyzes the homologous-pairing and strand-exchange reactions (8–11). In eukaryotes, two RecA homologues, the Rad51 and Dmc1 proteins, have been identified (12,13). The Rad51 protein is expressed in both meiotic and mitotic cells (14,15), but the Dmc1 protein is only present in meiotic cells (16,17).

*To whom correspondence should be addressed. Tel: +81 3 5369 7315; Fax: +81 3 5367 2820; Email: kurumizaka@waseda.jp
Correspondence may also be addressed to Kunihiro Ohta. Tel: +81 3 5464 8834; Fax: +81 3 5464 8834; Email: kohta@bio.c.u-tokyo.ac.jp

Previous studies revealed that the Dmc1 protein promotes homologous pairing (18,19) and strand exchange (20,21) between ssDNA and dsDNA *in vitro*. As in *Dmc1*-deficient yeast (16), both the knockout and mutations of the *dmc1* gene in mice cause sterility, due to a defect in homologous recombination (22–24), suggesting that the homologous-pairing and strand-exchange activities of the Dmc1 protein are essential for meiotic recombination in mammals. Sequencing of candidate genes from a set of infertile patients identified an infertile woman homozygous for the human *DMC1-M200V* polymorphism (25,26), raising the question of whether this single nucleotide polymorphism (SNP) (NCBI rfSNP ID: rs2227914) may cause infertility by affecting the function of the human DMC1 protein.

In the present study, we determined the crystal structure of the human DMC1-M200V variant in the octameric-ring form. Biochemical analyses revealed that the human DMC1-M200V variant was moderately defective in catalyzing *in vitro* recombination reactions, probably due to its reduced stability. Consistently, genetic analyses with the corresponding M194V mutation in the *Schizosaccharomyces pombe dmc1* gene caused a significant decrease in the meiotic homologous recombination frequency. In addition, we found that the Arg252 residue, which may interact with the Met200 residue in the human DMC1 protomer, is involved in dsDNA binding. These results suggested that the region around the Met200 residue is important for the function of the human DMC1 protein during meiosis.

METHODS

Purification of the human DMC1 protein and the DMC1 mutants

The human DMC1 protein, the DMC1-M200V variant, the DMC1-M249V mutant, the DMC1-R252G mutant and the DMC1-R252S mutant were each overexpressed with the pET-15b plasmid system (Novagen, Darmstadt, Germany) in the *E. coli* strain BL21(DE3) Codon Plus (Stratagene, La Jolla, CA, USA), as hexahistidine-tagged proteins. The proteins were then purified by the method described previously (27). Briefly, the cells producing the proteins were harvested and were lysed by sonication in buffer A [50 mM Tris–HCl buffer (pH 8.0), containing 0.5 M NaCl, 2 mM 2-mercaptoethanol, 10% glycerol and 5 mM imidazole] on ice. The cell lysate was centrifuged at $27\,700 \times g$ for 20 min, and the supernatant was gently mixed by the batch method with 4 ml of Ni-NTA agarose beads (Qiagen, Hilden, Germany) at 4°C for 1 h. The protein-bound beads were packed into an Econo-column (Bio-Rad Laboratories, Hercules, CA, USA) and were washed with 30 column volumes of buffer A. The human DMC1 protein was eluted in a 20 column-volume linear gradient of 5–500 mM imidazole in buffer A. The peak fractions were collected, and thrombin protease (2 U/mg of the human DMC1 protein; GE Healthcare Biosciences, Uppsala, Sweden) was added to remove the His-tag. The samples were then immediately dialyzed overnight at 4°C in buffer B [20 mM Tris–HCl buffer (pH 8.0), containing 0.2 M KCl, 0.25 mM EDTA, 2 mM 2-mercaptoethanol and 10% glycerol]. The human DMC1 protein, which now lacked the His-tag, was subjected to chromatography on a 4 ml Heparin–Sepharose (GE Healthcare Biosciences) column. The column was washed with 20 column volumes of buffer B, and the protein was eluted with a 20 column-volume linear gradient of 0.2–1.0 M KCl in buffer B. The purified proteins were concentrated with a Centricon Ultracel YM-30 filter (Amicon, Millipore, Billerica, MA, USA), and the buffer was exchanged with 20 mM HEPES–KOH buffer (pH 7.5), containing 500 mM KCl, 0.25 mM EDTA, 2 mM 2-mercaptoethanol and 10% glycerol. The protein concentration was determined using the Bradford method, with bovine serum albumin (Pierce, Rockford, IL, USA) as the standard.

Crystallization, structure determination and refinement

The human DMC1-M200V crystals were grown by the hanging drop method at 20°C. The hanging drop was formed by adding 1 μl of the human DMC1-M200V variant (concentrated to 8 mg/ml) to 1 μl of the reservoir solution [0.1 M sodium citrate buffer (pH 5.5) containing 50 mM $MgCl_2$ and 9% PEG 2000 MME]. Crystals typically appeared after 1 week, and reached the maximum size (0.5 mm × 0.5 mm × 0.05 mm) after 2 weeks. For data collection, the human DMC1-M200V crystals were harvested in a reservoir solution containing 30% PEG 400, and were flash-cooled in a stream of N_2 gas (100 K). The data set of the crystal was collected at the SPring-8 BL26B2 beamline (Harima, Japan). The data were reduced using the DENZO and SCALEPACK programs (28). The crystals of the human DMC1-M200V variant belong to the tetragonal space group of I422, with unit cell dimensions $a = b = 124.09$ Å and $c = 217.87$ Å. The structure of the human DMC1-M200V variant was determined by molecular replacement, using the MOLREP program (29). The coordinates of the human DMC1 structure (Protein Data Bank accession number 1V5W) were used as a search model without resetting the B-factors. The structure of the human DMC1-M200V variant was subjected to rigid body, energy minimization and B-factor refinements with the CNS program, using a 2-fold non-crystallographic symmetry (NCS) restraint (30). The Ramachandran plot of the final structure showed 79.3% of the residues in the most favorable regions and no residues in the disallowed region. All structure figures were created using the PyMOL program (31).

DNA substrates

In the D-loop formation assay, alkaline treatment of the cells harboring the plasmid DNA was avoided, to prevent the dsDNA substrates from undergoing irreversible denaturation. Instead, the cells were gently lysed using sarkosyl, as described previously (32). The pGsat4 DNA was created by inserting a 198-bp fragment of the human satellite-4 sequence into the pGEM-T easy vector (Promega, Madison, WI, USA) (33). For the ssDNA substrate used in the D-loop assay, the following high-performance liquid chromatography (HPLC)-purified oligonucleotide

was purchased from Roche Applied Science: 50-mer, 5′-ATT TCA TGC TAG ACA GAA GAA TTC TCA GTA ACT TCT TTG TGC TGT GTG TA-3′. The 5′ ends of the oligonucleotides were labeled with T4 polynucleotide kinase (New England Biolabs, Ipswich, MA, USA) in the presence of $[\gamma\text{-}^{32}P]ATP$ at 37°C for 30 min. DNA concentrations are expressed in moles of nucleotides.

The D-loop assay

The reactions were conducted in 10 μl of 20 mM Tris–HCl buffer (pH 8.0), containing 1 mM ATP, 2 mM creatine phosphate, 75 μg/ml creatine kinase and 0.1 mg/ml bovine serum albumin, and were started by incubating the indicated amounts of the human DMC1 protein, the DMC1-M200V variant or the DMC1-M249V mutant with 1 μM of ^{32}P-labeled ssDNA 50-mer at 37°C for 5 min. Afterwards, the supercoiled dsDNA (pGsat4; final concentration of 30 μM) was added along with $MgCl_2$ (final concentration of 1–5 mM). The reaction mixtures were further incubated for the indicated times. The reactions were terminated by the addition of 0.5% SDS and 0.6 mg/ml proteinase K (Roche Applied Science, Basel, Switzerland), and the samples were further incubated at 37°C for 15 min. The products were resolved by 1% agarose gel electrophoresis in 0.5 × TBE buffer at 3.3 V/cm for 2.5 h, and were visualized and quantitated by a BAS-2500 imaging analyzer (Fujifilm, Tokyo, Japan) equipped with the Image Gauge software.

The strand-exchange assay

The human DMC1 protein, the DMC1-M200V variant, the DMC1-M249V mutant, the DMC1-R252G mutant or the DMC1-R252S mutant was incubated with 20 μM ϕX174 circular ssDNA at 37°C (or 42 or 47°C), for 10 min, in 10 μl of 20 mM HEPES–KOH buffer (pH 7.5), containing 1 mM ATP, 1 mM $MgCl_2$, 0.1 mg/ml bovine serum albumin, 20 mM creatine phosphate and 75 μg/ml creatine kinase. After this incubation, 2 μM RPA and the indicated amount of KCl were added to the reaction mixture, which was incubated at 37°C (or 42 or 47°C) for 10 min. The reactions were then initiated by the addition of 20 μM ϕX174 linear dsDNA and were continued for 1 h. The reactions were stopped by the addition of 0.1% SDS and 1.7 mg/ml proteinase K (Roche Applied Science), and the samples were further incubated at 37°C for 20 min. The deproteinized reaction products were separated by 1% agarose gel electrophoresis in 1 × TAE buffer (ice-cold, 40 mM Tris–acetate and 1 mM EDTA) at 3.0 V/cm for 4 h. The products were visualized by SYBR Gold (Invitrogen, Carlsbad, CA, USA) staining.

Circular dichroism (CD) measurements

The CD spectra of the human DMC1 protein (2 μM) and the DMC1 mutants (2 μM) were measured on a JASCO J-820 spectropolarimeter (Japan Spectroscopic Co., Ltd, Tokyo, Japan) using a 1 cm pathlength quartz cell. All of the CD experiments were performed in 20 mM potassium phosphate (pH 7.0) and 50 mM KCl.

Assays for DNA binding

The ϕX174 circular ssDNA (20 μM) or the supercoiled ϕX174 dsDNA (10 μM) was mixed with the human DMC1 protein or the DMC1 mutants in 10 μl of a standard reaction solution, containing 20 mM HEPES–KOH (pH 7.5), 1 mM DTT, 0.1 mg/ml bovine serum albumin, 1 mM $MgCl_2$, 250 mM KCl, 5% glycerol and 1 mM ATP. The reaction mixtures were incubated at 37°C for 10 min, and were then analyzed by 0.8% agarose gel electrophoresis in 1 × TAE buffer at 3.3V/cm for 3 h. The bands were visualized by ethidium bromide staining.

ATPase activity

The human DMC1 protein, the DMC1-M200V variant or the DMC1-M249V mutant was incubated with 1 mM ATP (Roche, ATP sodium salt) in 20 mM HEPES–KOH (pH 7.5), 125 mM KCl, 1 mM $MgCl_2$, 1 mM dithiothreitol and 0.1 mg/ml bovine serum albumin, in the presence of 1.5 M NaCl. The reaction was performed at 37, 42 and 47°C. After a 10 min preincubation in the absence of ATP, the reaction was initiated by adding 1 mM ATP. At the indicated times, a 20 μl aliquot of the reaction mixture was mixed with 30 μl of 100 mM EDTA to quench the reaction. The amount of inorganic phosphate released was determined by a colorimetric assay, as described previously (34).

Measurement of meiotic recombination frequency in *S. pombe*

Each haploid strain, h^+ *ade6-M26 his5-303* and h^- *ade6-469 leu1-32* carrying the *dmc1* mutation (*dmc1△*, M194V, M242V or M194/242V), was grown on a yeast extract plate (YE) (35) supplemented with adenine (100 mg/l) at 30°C. Equal volumes of each strain were mixed in 50 μl of a leucine solution (10 mg/ml), spotted on sporulation medium agar (SPA) plates (36) and incubated at 30°C for 3 days to allow mating and sporulation. The sporulating cells were suspended in 700 μl of 0.5% glusulase and were agitated at 30°C for 30 min. After this incubation, a 300 μl aliquot of ethanol was added to kill the surviving cells. The suspensions were centrifuged and the pellets were washed with dH_2O. Appropriate numbers of spores were spread onto SD (37) lacking leucine and histidine, SD lacking adenine or YE containing adenine. The recombination frequency was calculated from the number of colonies on the SD-Leu-His plate, the SD-Ade plate and the YE + Ade plate (for intergenic recombination Leu^+His^+(%), for intragenic recombination Ade^+/1000 spores). For each cross, over 10^4 and 10^5 spores were analyzed for intergenic and intragenic recombination, respectively. The spore viability was not affected in all of the mutants created in this study, which is consistent with the fact that Dmc1 is not essential for spore viability, as previously shown (38).

Accession codes

Protein Data Bank: The coordinates have been deposited, with the accession code 2ZJB.

RESULTS

The crystal structure of the human DMC1-M200V variant

In humans, genome-wide SNP analyses identified several variations of the *human DMC1* gene, including the M200V polymorphism, in which the Met200 residue is replaced by Val. This variant is present in the human population in the heterozygous state (*DMC1-M200V/DMC1*) with an average frequency of 0.22, with rare homozygous individuals (NCBI rfSNP ID: rs2227914). Intriguingly, one case of a homozygous substitution, 33551 A > G (sequence AY520538 in Genbank), has been found in the tenth exon, leading to the human DMC1-M200V change, in the analysis of the *human DMC1*-coding sequence in a panel of infertile patients (25,26).

To elucidate the molecular consequences of this single point mutation, we purified and crystallized the full-length human DMC1-M200V variant. The structure of the central ATPase domain of the DMC1-M200V variant was solved at 3.5 Å resolution by the molecular replacement method, using the human DMC1 structure as a guide (Table 1). The human DMC1-M200V variant was crystallized in an octameric ring form, like that of the human DMC1 protein (27) (Figure 1A). The Val200 residue is located near the middle of the α-11 helix, and its side-chain faces toward the hydrophobic core of the human DMC1-ATPase domain created by the Met249 residue (Figure 1B). In the DMC1-M200V variant, the side-chain atoms of the Val200 residue were approximately 4 Å away from the side-chain atoms of the Met249 residue, indicating that hydrophobic interactions

Table 1. Data collection and refinement statistics

Data collection	
Space group	*I*422
Cell dimensions	
a, *b*, *c* (Å)	124.09, 124.09, 217.87
Resolution (Å)	50.0–3.5 (3.63–3.5)[a]
Rsym (%)	8.5 (46.4)
$I/\sigma I$	9.4 (6.0)
Completeness (%)	100 (100)
Redundancy	13.1 (13.8)
Refinement	
Resolution (Å)	20.0 (3.5)
Number of reflections	11 034 (1 138)[b]
R_{work}/R_{free} (%)	29.4/35.1
R.m.s. deviations	
Bond lengths (Å)	0.008
Bond angles (°)	1.32

[a]Highest-resolution shell shown in parentheses.
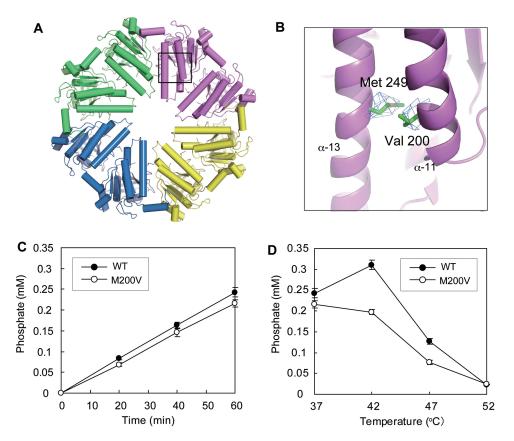[b]Number of test reflections shown in parentheses.

Figure 1. The crystal structure of the human DMC1-M200V variant. (**A**) The octameric ring structure of the human DMC1-M200V variant. Each color represents an asymmetric unit. (**B**) A close-up view of the boxed region in (A), which contains the Val200 and Met249 residues. The Val200 and Met249 residues are located on the α-11 and α-13 helices, respectively. The simulated annealing $2F_o - F_c$ omit map, calculated without the coordinates of Val200 and Met249, is shown in blue. The electron density is contoured at 1.0 σ. (**C**) Salt-induced ATPase activities. Graphic representation of the time-course experiments at 37°C. (**D**) Temperature dependence of salt-induced ATPase activities. The reactions were performed at 37, 42 and 47°C for 1 h. Closed circles and open circles indicate the experiments with the human DMC1 protein and the DMC1-M200V variant, respectively.

were still present between the two residues (Figure 1B). These interactions bridge the α-11 and α-13 helices, and therefore, the replacement with the Val residue, which has a smaller hydrophobic surface area than the Met residue, could destabilize α-11 and α-13, making them more mobile than those in the conventional human DMC1 protein.

To compare the stability of the human DMC1-M200V variant and the human DMC1 protein, the ATPase activity was examined under elevated temperature conditions. The human DMC1 protein hydrolyzes ATP in the presence of either DNA or a high salt concentration. To evaluate the stability of the DMC1-M200V variant, we employed the salt-induced ATPase assay, because the DNA-binding activity may also be affected under higher temperature conditions. As shown in Figure 1C, the DMC1-M200V variant hydrolyzed ATP to the same extent as the human DMC1 protein in the presence of 1.5 M NaCl at 37°C. The human DMC1 protein exhibited enhanced ATPase activity at 42°C. However, this enhancement was not observed with the DMC1-M200V variant (Figure 1D). In addition, the ATPase activity of the human DMC1-M200V variant was clearly lower than that of the human DMC1 protein at 47°C (Figure 1D). These results demonstrated the reduced stability of the DMC1-M200V variant, as compared to the conventional human DMC1 protein.

Defective homologous pairing by the human DMC1-M200V variant

We then examined the homologous-pairing activity of the human DMC1-M200V variant. To do so, we employed the D-loop formation assay, which was used to detect the homologous-pairing activity of the human DMC1 and yeast Dmc1 proteins (18,19). In this assay, a single-stranded oligonucleotide and superhelical dsDNA are used as substrates, and the D-loop is formed as a product of the homologous-pairing reaction (Figure 2A). When the D-loop assay was performed in the presence of 1–3 mM Mg^{2+}, the human DMC1-M200V variant was clearly defective in homologous pairing (Figure 2B, lanes 2–7). The homologous-pairing defect of the variant was not obvious at higher, non-physiological Mg^{2+} concentrations, such as 4 and 5 mM (Figure 2B, lanes 8–11). To confirm the homologous-pairing defect of the variant under low Mg^{2+} conditions, we performed time-course and protein titration experiments in the presence of 3 mM Mg^{2+}. The human DMC1-M200V variant was clearly defective in homologous pairing under the 3 mM Mg^{2+} conditions, as compared to the human DMC1 protein (Figure 2C and D). These results indicated that the DMC1-M200V variant is defective in homologous pairing under limited conditions, such as at low Mg^{2+} concentrations.

Strand-exchange activity of the human DMC1-M200V variant

In the time-course experiment, the amount of D-loops formed by the human DMC1 protein increased up to 10 min, and then the D-loops gradually dissociated afterwards (Figure 2C). While the DMC1-M200V variant was defective in promoting D-loop formation, it was proficient
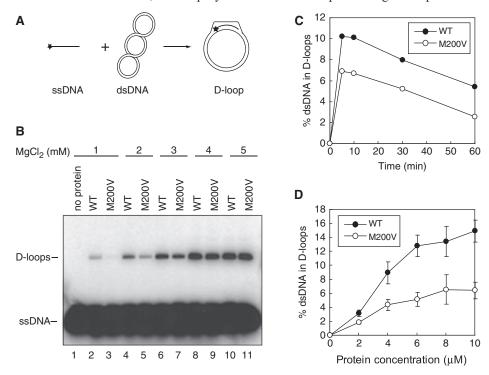
Figure 2. The human DMC1-M200V variant is defective in homologous pairing. (**A**) A schematic diagram of the D-loop formation assay. Asterisks indicate the ^{32}P-labeled end of the 50-mer ssDNA. (**B**) The reactions were conducted with the human DMC1 protein (4 μM) or the DMC1-M200V variant (4 μM) in the presence of the indicated amount of $MgCl_2$, and were continued for 10 min. (**C**) Graphic representation of the time-course experiments. Closed and open circles indicate the experiments with the human DMC1 protein (4 μM) and the DMC1-M200V variant (4 μM), respectively. (**D**) Graphic representation of the protein titration experiments at 10 min. Closed and open circles indicate the experiments with the human DMC1 protein and the DMC1-M200V variant, respectively.

in dissociating D-loops (Figure 2C). Since D-loop dissociation is a consequence of DNA strand exchange (39,40), these results suggest that the DMC1-M200V variant may be proficient in strand exchange. To test this possibility, we performed a strand-exchange assay using φX174 phage circular ssDNA (5386 bases) and linearized φX174 dsDNA (5386 bps) as DNA substrates. Both intermediate (joint molecule; JM) and complete strand-exchange products (nicked circular; NC) are detectable in this assay (Figure 3A).

We found that the strand-exchange activity of the human DMC1-M200V variant was similar to that of the human DMC1 protein at 37°C in the presence of 200 mM KCl, which is required to efficiently promote the strand-exchange reaction (Figure 3B, lanes 1–7). Similar results were obtained, when the strand-exchange assay was performed at 42°C (Figure 3B, lanes 8–14). These results suggest that the DMC1-M200V variant has robust strand-exchange activity, in spite of its moderately reduced homologous-pairing activity.

When the strand-exchange assay was performed at 47°C, the JM intermediate was still formed by 15 μM of the human DMC1 protein (Figure 3B, lane 18). In contrast, the strand-exchange activity of the DMC1-M200V variant was quite defective at 47°C (Figure 3B, lanes 15–21). Consistently, the DMC1-M200V variant showed a clear defect in the ATPase activity at 47°C (Figure 1D). These results suggested that the reduced stability of the DMC1-M200V variant causes its defective recombinase activity.

Genetic analyses of the M194V mutation in the *S. pombe* Dmc1 protein

To evaluate the effect of the human DMC1-M200V mutation in living cells, which have other compensatory factors, such as the Rad51 protein, we next performed genetic analyses with the fission yeast, *S. pombe*. The Met200 residue of the human DMC1 protein is conserved in the *S. pombe* Dmc1 protein (Met194) (Figure 4A). Therefore, we introduced the M194V mutation in the *S. pombe* *dmc1*[+] gene and tested whether the mutation affected meiotic recombination. In *S. pombe*, complete null dmc1Δ mutants still exhibit background levels of recombination in meiosis: about 20% of the wild-type levels of the intergenic recombination frequency between *leu1-his5* and the intragenic gene conversion at *ade6-M26/ade6-M469*. As shown in Figure 4B and C, the M194V mutation conferred a reduction in both types of recombination (nearly half of the wild-type level). The M242V mutation, which corresponds to the Met249 residue of the human DMC1 protein, was introduced in the *S. pombe* *dmc1*[+] gene. The Met249 residue is embedded within the hydrophobic core of the human DMC1–ATPase domain, and directly interacts with the Met200 residue in the human DMC1 structure. The M249V mutation in the human DMC1 protein significantly impaired both homologous pairing and strand exchange (Figure 4D and E). The corresponding mutation in *S. pombe* caused a drastic reduction in both types of meiotic recombination, down to the null mutant levels (Figure 4B and C). Therefore, the M194V and M242V alleles in the *S. pombe* *dmc1*[+] gene
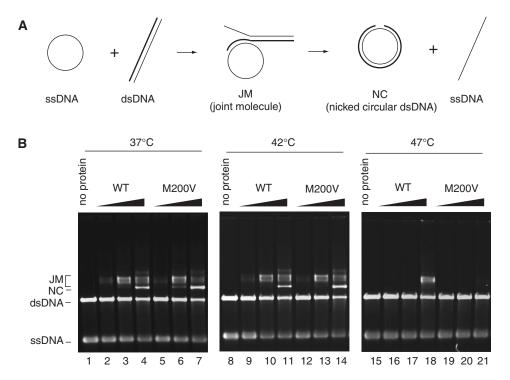

Figure 3. The strand-exchange activity of the human DMC1-M200V variant. (**A**) A schematic diagram of the strand-exchange assay. (**B**) Temperature dependence of the strand-exchange activities. The samples were incubated at 37°C (lanes 1–7), 42°C (lanes 8–14) and 47°C (lanes 15–21) for 1 h in the presence of 200 mM KCl. Lanes 1, 8 and 15 indicate control experiments without the human DMC1 protein. Lanes 2–4, 9–11 and 16–18 indicate experiments with the human DMC1 protein and lanes 5–7, 12–14 and 19–21 indicate experiments with the DMC1-M200V variant. The protein concentrations were 3.75 μM (lanes 2, 5, 9, 12, 16 and 19), 7.5 μM (lanes 3, 6, 10, 13, 17 and 20) and 15 μM (lanes 4, 7, 11, 14, 18 and 21).

are reduction-of-function and loss-of-function mutations, respectively. The M194V and M242V double mutation displayed a recombination defect similar to those of the M242V mutant and the *dmc1* Δ mutant (Figure 4B and C). These results revealed a parallel correlation between the *in vitro* homologous-pairing deficiencies of the human DMC1-M200V variant and the DMC1-M249V mutant.

The Arg252 residue is involved in DNA binding by the human DMC1 protein

In the human DMC1 structure, we next searched for the amino acid residues that may be affected by the M200V substitution. The Arg252 residue was a likely candidate, because this residue is located at a position where its β- and γ-CH_2 groups could interact with the Met200 residue in the conventional human DMC1 protein. The human DMC1-R252S and DMC1-R252G mutants were then purified. A CD spectroscopic analysis revealed that the mutations did not disrupt the secondary structures of the proteins (Figure 5A). As shown in Figure 5B, both the DMC1-R252S and DMC1-R252G mutants were significantly defective in the strand-exchange activity, suggesting a problem with DNA binding. Intriguingly, the ssDNA-binding activities of the DMC1-R252S and DMC1-R252G mutants were proficient, although that of the DMC1-R252S mutant was slightly reduced (Figure 5C). However, the dsDNA-binding activities of both mutants were clearly defective, as compared to that of the human DMC1 protein (Figure 5D). Since the Arg252 residue is exposed on the surface of the human DMC1 protein, this residue may function as a DNA-binding residue that is specific for dsDNA.

DISCUSSION

Genome-wide SNP analyses revealed the presence of the human *DMC1-M200V* polymorphism in the human population, in the heterozygous state (*DMC1-M200V/DMC1*) with an average frequency of 0.22 and with rare homozygous individuals. An infertile woman, who is homozygous for the human *DMC1-M200V* polymorphism, has been identified in a set of infertile patients (25,26), suggesting that this polymorphism may cause infertility by affecting the structure and function of the human DMC1 protein. To test this possibility, we purified and crystallized the human DMC1-M200V protein. A significant structural change was not found in the DMC1-M200V variant, but our biochemical analyses indicated that the variant was less stable, as compared to the conventional human DMC1 protein. Intriguingly, the DMC1-M200V variant was moderately defective in catalyzing *in vitro* recombination reactions, and the corresponding M194V mutation in the *S. pombe* *dmc1*+ gene also caused a significant decrease in the meiotic homologous recombination frequency *in vivo*. These structural, biochemical and genetic results obtained in this study strongly suggested that the human *DMC1-M200V* polymorphism causes a partial defect in the function of the DMC1 protein during meiosis. Since the homozygous human *DMC1-M200V* polymorphism was found in an infertile woman, it might be responsible for a class of premature ovarian failure (POF, OMIM#311360) disorder (25,26), due to defective meiotic homologous recombination. In order to confirm that the homozygous *DMC1-M200V* polymorphism is a source of human infertility, comprehensive analyses of the *DMC1* polymorphism in infertile patients and further studies to
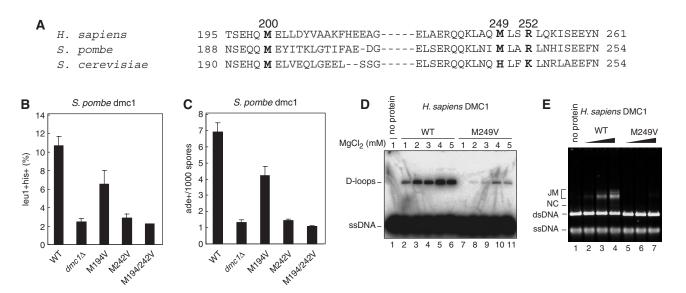

Figure 4. The M194V and M242V mutations in the *S. pombe* *dmc1* gene cause recombination defects in meiosis. (**A**) Sequence alignment of the human DMC1 Met200 and Met249 residues with the *S. pombe* and *Saccharomyces cerevisiae* Dmc1 proteins. (**B** and **C**) The M194V and M242V mutations in the *S. pombe* *dmc1* gene affect intergenic and intragenic recombination in meiosis. Intergenic recombination between *leu1-32* and *his5-303* and intragenic recombination within the *ade6* gene (*ade6-M26 and ade6-469*) were measured. Rates of intergenic recombination and intragenic recombination are indicated as leu + his + (%) (in **B**) and ade + /1000 spores (in **C**), respectively. (**D**) The human DMC1-M249V mutant is defective in homologous pairing, the D-loop assay. The reactions were conducted with the human DMC1 protein (4 μM) or the DMC1-M249V mutant (4 μM) in the presence of the indicated amount of $MgCl_2$, and were continued for 10 min. (**E**) The human DMC1-M249V mutant is defective in strand exchange. The reactions were conducted with the human DMC1 protein (3.75, 7.5 and 15 μM) and the DMC1-M249V mutant for 1 h.
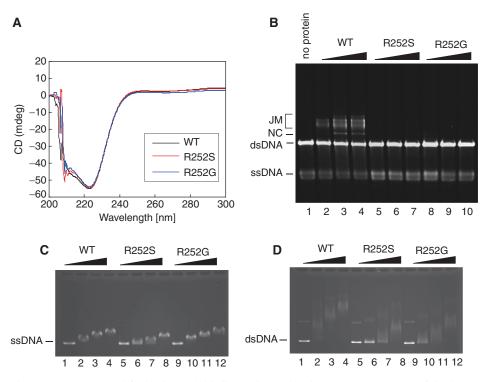
Figure 5. The R252S and R252G mutants are defective in DNA binding and strand exchange. (**A**) CD spectra of the human DMC1 protein ($2 \mu M$, black line), the DMC1-R252G mutant ($2 \mu M$, blue line) and the DMC1-R252S mutant ($2 \mu M$, red line) were recorded at $25°C$. (**B**) The strand-exchange assay. The protein concentrations were $3.75 \mu M$ (lanes 2, 5 and 8), $7.5 \mu M$ (lanes 3, 6 and 9) and $15 \mu M$ (lanes 7 and 10). Lanes 2–4, 5–7 and 8–10 indicate experiments with the human DMC1 protein, the DMC1-R252S mutant and the DMC1-R252G mutant, respectively. The reactions were carried out for 1 h. (**C**) The ssDNA-binding experiments. The $\phi X174$ circular ssDNA ($20 \mu M$) was incubated with the human DMC1 protein, the DMC1-R252S mutant or the DMC1-R252G mutant at $37°C$ for 10 min. (**D**) The dsDNA-binding experiments. The supercoiled dsDNA ($10 \mu M$) was incubated with the human DMC1 protein, the DMC1-R252S mutant or the DMC1-R252G mutant at $37°C$ for 10 min. The protein concentrations were $3.75 \mu M$ (lanes 2, 5 and 8), $7.5 \mu M$ (lanes 3, 6 and 9) and $15 \mu M$ (lanes 4, 7 and 10).

determine whether the M200V mutation in the mouse DMC1 protein also causes infertility will be required.

The human DMC1 protein is known to form octameric ring (27,41,42) and helical filament (20) structures, and the helical filament is considered to be the active form for the recombinase activities, such as homologous pairing and strand exchange (20,21). Among the DMC1 homologs, the crystal structures of the archaeal RadA and yeast Rad51 filaments have been reported (43–46), and the human DMC1 and *S. pombe* Dmc1 proteins appear to form similar filament structures as those of the Rad51 protein (20,47). In the crystal structure of the archaeal RadA protein, the α-helix corresponding to the α-13 helix of the human DMC1 protein contains the Asp246 residue that binds to Mg^{2+}. This Mg^{2+} ion is also bound by several residues from the neighboring protomer, and could be essential for the formation of the active filament structure (48). Therefore, mutations in the α-helix harboring these residues may alter the structure of the metal-binding site. Given that the α-13 helix of the human DMC1 protein contains the putative Mg^{2+}-binding residue, the M200V mutation may have affected the Mg^{2+} ion binding, because the Met200 residue forms direct hydrophobic interactions with the Met249 residue of the α-13 helix. Therefore, the human DMC1-M200V mutation may partially impair the Mg^{2+} ion-dependent formation of the active filament structure. Consistent

with this view, the human DMC1-M200V mutant was defective in homologous pairing at low Mg^{2+} concentrations, but was nearly proficient at higher concentrations (Figure 2B). Thus, the M200V mutation may also affect the Mg^{2+}-binding site, in addition to the thermostability of the human DMC1 protein. Interestingly, the DMC1 residue corresponding to the RadA-Asp246 residue is Glu258, which engages in tripartite hydrogen bonding with residues in the neighboring protomer. This residue was demonstrated to be essential for the stabilization of the ring structure (27). The Glu258 residue may have a dual mode of interaction, by either binding to Mg^{2+} in the helical filament form or engaging in the tripartite hydrogen bonding in the ring form.

Finally, we and others (49–51) previously suggested that a DNA-binding (HhH) motif, located in the N-terminal domain of the Rad51 or RadA protein, constitutes a DNA-binding path that runs between two consecutive N-terminal domains in the filament structure (Figure 6), and functions to guide DNA to the DNA-binding loops, L1 and L2, which are located inside the filament. It is possible that the corresponding region of the DMC1 protein also functions similarly. Interestingly, the α-11 and α-13 helices, which contain the Met200 and Met249/Arg252 residues, respectively, are located in this putative DNA-binding path. Our present finding that the Arg252 residue on the α-13 helix is important for the
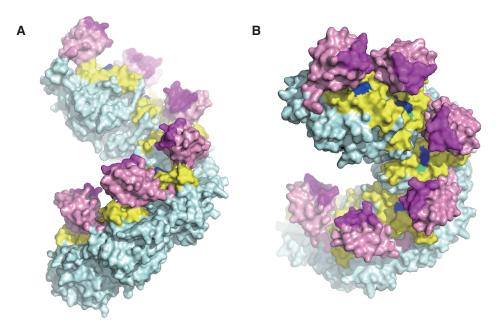
Figure 6. The corresponding locations of the human DMC1-Met200 and DMC1-Arg252 residues on the active RadA filament. One helical turn (composed of six molecules) of the RadA filament structure (34) (PDB ID: 1XU4) viewed from the side (**A**) and the top (**B**). Coloring is as follows: N-terminal domain (light pink), DNA-binding HhH motif (magenta), and α-11 and α-13 helices (yellow). The *Methanococcus voltae* RadA residues corresponding to human DMC1-Met200 and DMC1-Arg252 are Met189 and Thr240, respectively. The Thr240 residue was replaced by the corresponding Arg residue of the human DMC1 protein using the PyMOL program (42), and the Met189 and Arg240 residues are colored green and blue, respectively.

DNA-binding and strand-exchange activities of the human DMC1 protein supports this view. Thus, it is tempting to speculate that the M200V mutation directly affects the recombination activities of the human DMC1 protein. Structural studies of the human DMC1 filament bound to DNA should help unveil the role of the Met200 residue.

REFERENCES

1. Petronczki,M., Siomos,M.F. and Nasmyth,K. (2003) Un ménage à quatre: the molecular biology of chromosome segregation in meiosis. *Cell*, **112**, 423–440.

2. Bishop,D.K. and Zickler,D. (2004) Early decision: meiotic crossover interference prior to stable strand exchange and synapsis. *Cell*, **117**, 9–15.

3. Keeney,S., Giroux,C.N. and Kleckner,N. (1997) Meiosis-specific DNA double-strand breaks are catalyzed by Spo11, a member of a widely conserved protein family. *Cell*, **88**, 375–384.

4. Bergerat,A., de Massy,B., Gadelle,D., Varoutas,P.C., Nicolas,A. and Forterre,P. (1997) An atypical topoisomerase II from archaea with implications for meiotic recombination. *Nature*, **386**, 414–417.

5. Neale,M.J., Pan,J. and Keeney,S. (2005) Endonucleolytic processing of covalent protein-linked DNA double-strand breaks. *Nature*, **436**, 1053–1057.

6. Neale,M.J. and Keeney,S. (2006) Clarifying the mechanics of DNA strand exchange in meiotic recombination. *Nature*, **442**, 153–158.

7. Bishop,D.K. (2006) Multiple mechanisms of meiotic recombination. *Cell*, **127**, 1095–1097.

8. Shibata,T., DasGupta,C., Cunningham,R.P. and Radding,C.M. (1979) Purified Escherichia coli recA protein catalyzes homologous pairing of superhelical DNA and single-stranded fragments. *Proc. Natl Acad. Sci. USA*, **76**, 1638–1642.

9. McEntee,K., Weinstock,G.M. and Lehman,I.R. (1979) Initiation of general recombination catalyzed in vitro by the recA protein of Escherichia coli. *Proc. Natl Acad. Sci. USA*, **76**, 2615–2619.

10. Cox,M.M. and Lehman,I.R. (1981) Directionality and polarity in recA protein-promoted branch migration. *Proc. Natl Acad. Sci. USA*, **78**, 6018–6022.

11. Kahn,R., Cunningham,R.P., DasGupta,C. and Radding,C.M. (1981) Polarity of heteroduplex formation promoted by Escherichia coli recA protein. *Proc. Natl Acad. Sci. USA*, **78**, 4786–4790.

12. Masson,J.-Y. and West,S.C. (2001) The Rad51 and Dmc1 recombinases: a non-identical twin relationship. *Trends Biochem. Sci.*, **26**, 131–136.

13. Sehorn,M.G. and Sung,P. (2004) Meiotic recombination: an affair of two recombinases. *Cell Cycle*, **3**, 1375–1377.

14. Shinohara,A., Ogawa,H. and Ogawa,T. (1992) Rad51 protein involved in repair and recombination in *S. cerevisiae* is a RecA-like protein. *Cell*, **69**, 457–470.

15. Shinohara,A., Ogawa,H., Matsuda,Y., Ushio,N., Ikeo,K. and Ogawa,T. (1993) Cloning of human, mouse and fission yeast

recombination genes homologous to *RAD51* and *recA*. *Nat. Genet.*, **4**, 239–243.

16. Bishop,D.K., Park,D., Xu,L. and Kleckner,N. (1992) DMCI: a meiosis-specific yeast homolog of *E. coli* recA required for recombination, synaptonemal complex formation, and cell cycle progression. *Cell*, **69**, 439–456.

17. Habu,T., Taki,T., West,A., Nishimune,Y. and Morita,T. (1996) The mouse and human homologs of DMC1, the yeast meiosis-specific homologous recombination gene, have a common unique form of exon-skipped transcript in meiosis. *Nucleic Acids Res.*, **24**, 470–477.

18. Li,Z., Golub,E.I., Gupta,R. and Radding,C.M. (1997) Recombination activities of HsDmc1 protein, the meiotic human homolog of RecA protein. *Proc. Natl Acad. Sci. USA*, **94**, 11221–11226.

19. Hong,E.L., Shinohara,A. and Bishop,D.K. (2001) *Saccharomyces cerevisiae* Dmc1 protein promotes renaturation of single-strand DNA (ssDNA) and assimilation of ssDNA into homologous supercoiled duplex DNA. *J. Biol. Chem.*, **276**, 41906–41912.

20. Sehorn,M.G., Sigurdsson,S., Bussen,W., Unger,V.M. and Sung,P. (2004) Human meiotic recombinase Dmc1 promotes ATP-dependent homologous DNA strand exchange. *Nature*, **429**, 433–437.

21. Bugreev,D.V., Golub,E.I., Stasiak,A.Z., Stasiak,A. and Mazin,A.V. (2005) Activation of human meiosis-specific recombinase Dmc1 by Ca^{2+}. *J. Biol. Chem.*, **280**, 26886–26895.

22. Pittman,D.L., Cobb,J., Schimenti,K.J., Wilson,L.A., Cooper,D.M., Brignull,E., Handel,M.A. and Schimenti,J.C. (1998) Meiotic prophase arrest with failure of chromosome synapsis in mice deficient for *Dmc1*, a germline-specific RecA homolog. *Mol. Cell*, **1**, 697–705.

23. Yoshida,K., Kondoh,G., Matsuda,Y., Habu,T., Nishimune,Y. and Morita,T. (1998) The mouse *RecA*-like gene *Dmc1* is required for homologous chromosome synapsis during meiosis. *Mol. Cell*, **1**, 707–718.

24. Bannister,A.A., Pezza,R.J., Donaldson,J.R., de Rooij,D.G., Schimenti,K.J., Camerini-Otero,R.D. and Schimenti,J.C. (2007) A dominant, recombination-defective allele of Dmc1 causing male-specific sterility. *PLoS Biol.*, **5**, 1–10.

25. Mandon-Pépin,B., Derbois,C., Matsuda,F., Cotinot,C., Wolgemuth,D.J., Smith,K., McElreavey,K., Nicolas,A. and Fellous,M. (2002) Human infertility: meiotic genes as potential candidates. *Gynecol. Obstet. Fertil.*, **30**, 817–821.

26. Mandon-Pépin,B., Touraine,P., Kuttenn,F., Derbois,C., Rouxel,A., Matsuda,F., Nicolas,A., Cotinot,C. and Fellous,M. (2008) Genetic investigation of four meiotic genes in women with premature ovarian failure. *Eur. J. Endocrinol.*, **158**, 107–115.

27. Kinebuchi,T., Kagawa,W., Enomoto,R., Tanaka,K., Miyagawa,K., Shibata,T., Kurumizaka,H. and Yokoyama,S. (2004) Structural basis for octameric ring formation and DNA interaction of the human homologous-pairing protein Dmc1. *Mol. Cell*, **14**, 363–374.

28. Otwinowski,Z. and Minor,W. (1997) Processing of X-ray diffraction data collected in oscillation mode. *Methods Enzymol.*, **276**, 307–326.

29. CCP4, (1994) The CCP4 (Collaborative Computing Project 4) suite: programs for X-ray crystallography. *Acta Crystallogr. D*, **50**, 760–763.

30. Brunger,A.T., Adams,P.D., Clore,G.M., DeLano,W.L., Gros,P., Grosse-Kunstleve,R.W., Jiang,J.-S., Kuszewski,J., Nilges,M. and Pannu,N.S. (1998) Crystallography and NMR system: a new software suite for macromolecular structure determination. *Acta Crystallogr. D*, **54**, 904–925.

31. DeLano,W.L. (2002) *The PyMOL Molecular Graphics System*. DeLano Scientific, San Carlos, CA, USA.

32. Kagawa,W., Kurumizaka,H., Ikawa,S., Yokoyama,S. and Shibata,T. (2001) Homologous pairing promoted by the human Rad52 protein. *J. Biol. Chem.*, **276**, 35201–35208.

33. Tanaka,Y., Tawaramoto-Sasanuma,M., Kawaguchi,S., Ohta,T., Yoda,K., Kurumizaka,H. and Yokoyama,S. (2004) Expression and purification of recombinant human histones. *Methods*, **33**, 3–11.

34. Matsuo,Y., Sakane,I., Takizawa,Y., Takahashi,M. and Kurumizaka,H. (2006) Roles of the human Rad51 L1 and L2 loops in DNA binding. *FEBS J.*, **273**, 3148–3159.

35. Moreno,S., Klar,A. and Nurse,P. (1991) Molecular genetic analysis of fission yeast Schizosaccharomyces pombe. *Methods Enzymol.*, **194**, 795–823.

36. Gutz,H., Heslot,H., Leupold,U. and Loprieno,N. (1974) *Schizosaccharomyces pombe*. In King,R.D. (ed.), *Handbook of Genetics*, Vol. 1. Plenum, New York.

37. Sherman,F., Fink,G. and Hicks,J. (1986) *Methods in Yeast Genetics: Laboratory Course Manual*. Cold Spring Harbor Laboratory Press, Cold Spring Harbor, New York.

38. Fukushima,K., Tanaka,Y., Nabeshima,K., Yoneki,T., Tougan,T., Tanaka,S. and Nojima,H. (2000) Dmc1 of *Schizosaccharomyces pombe* plays a role in meiotic recombination. *Nucleic Acids Res.*, **28**, 2709–2716.

39. Shibata,T., Ohtani,T., Iwabuchi,M. and Ando,T. (1982) D-loop cycle. A circular reaction sequence which comprises formation and dissociation of D-loops and inactivation and reactivation of superhelical closed circular DNA promoted by recA protein of Escherichia coli. *J. Biol. Chem.*, **257**, 13981–13986.

40. Wu,A.M., Kahn,R., DasGupta,C. and Radding,C.M. (1982) Formation of nascent heteroduplex structures by RecA protein and DNA. *Cell*, **30**, 37–44.

41. Passy,S.I., Yu,X., Li,Z., Radding,C.M., Masson,J.Y., West,S.C. and Egelman,E.H. (1999) Human Dmc1 protein binds DNA as an octameric ring. *Proc. Natl Acad. Sci. USA*, **96**, 10684–10688.

42. Masson,J.-Y., Davies,A.A., Hajibagheri,N., Van Dyck,E., Benson,F.E., Stasiak,A.Z., Stasiak,A. and West,S.C. (1999) The meiosis-specific recombinase hDmc1 forms ring structures and interacts with hRad51. *EMBO J.*, **18**, 6552–6560.

43. Wu,Y., He,Y., Moya,I.A., Qian,X. and Luo,Y. (2004) Crystal structure of archaeal recombinase RadA: a snapshot of its extended conformation. *Mol. Cell*, **15**, 423–435.

44. Conway,A.B., Lynch,T.W., Zhang,Y., Fortin,G.S., Fung,C.W., Symington,L.S. and Rice,P.A. (2004) Crystal structure of a Rad51 filament. *Nat. Struct. Mol. Biol.*, **11**, 791–796.

45. Wu,Y., Qian,X., He,Y., Moya,I.A. and Luo,Y. (2005) Crystal structure of an ATPase-active form of Rad51 homolog from *Methanococcus voltae*. *J. Biol. Chem.*, **280**, 722–728.

46. Chen,L.-T., Ko,T.-P., Chang,Y.-C., Lin,K.-A., Chang,C.-S., Wang,A.H.-J. and Wang,T.-F. (2007) Crystal structure of the left-handed archaeal RadA helical filament: identification of a functional motif for controlling quaternary structures and enzymatic functions of RecA family proteins. *Nucleic Acids Res.*, **35**, 1787–1801.

47. Sauvageau,S., Stasiak,S.Z., Banville,I., Ploquin,M., Stasiak,A. and Masson,J.-Y. (2005) Fission Yeast Rad51 and Dmc1, two efficient DNA recombinases forming helical nucleoprotein filaments. *Mol. Cell. Biol.*, **25**, 4377–4387.

48. Qian,X., He,Y. and Luo,Y. (2007) Binding of a second magnesium is required for ATPase activity of RadA from *Methanococcus voltae*. *Biochemistry*, **46**, 5855–5863.

49. Aihara,H., Ito,Y., Kurumizaka,H., Yokoyama,S. and Shibata,T. (1999) The N-terminal domain of the human Rad51 protein binds DNA: structure and a DNA binding surface as revealed by NMR. *J. Mol. Biol.*, **290**, 495–504.

50. Shin,D.S., Pellegrini,L., Daniels,D.S., Yelent,B., Craig,L., Bates,D., Yu,D.S., Shivji,M.K., Hitomi,C., Arvai,A.S. *et al.* (2003) Full-length archaeal Rad51 structure and mutants: mechanisms for RAD51 assembly and control by BRCA2. *EMBO J.*, **22**, 4566–4576.

51. Chen,L.-T., Ko,T.-P., Chang,Y.-W., Lin,K.-A., Wang,A.H.-J. and Wang,T.-F. (2007) Structural and functional analyses of five conserved positively charged residues in the L1 and N-terminal DNA binding motifs of archaeal RadA protein. *PLoS one*, **9**, 1–11.